

000 001 E²AT: MULTIMODAL JAILBREAK DEFENSE VIA DY- 002 NAMIC JOINT OPTIMIZATION 003 004

005 **Anonymous authors**

006 Paper under double-blind review

007 008 ABSTRACT 009

011 Research endeavors have been made in learning robust Multimodal Large Lan-
012 guage Models (MLLMs) against jailbreak attacks. However, existing methods
013 for improving MLLMs’ robustness still face critical challenges: ① how to effi-
014 ciently tune massive weight parameters and ② how to ensure robustness against
015 attacks across both visual and textual modalities. To this end, we propose an
016 **Efficient End-to-end Adversarial Training (E²AT)** framework for both visual and
017 textual adversarial attacks. Specifically, for the visual aspect, E²AT incorporates
018 an efficient projector-based AT module that aligns the attack samples at the fea-
019 ture level. For training objectives, we propose a **Dynamic Joint Multimodal Opti-
020 mization (DJMO)** strategy to enhance generalization ability against jailbreak
021 attacks by dynamically adjusting weights between normal and adversarial ob-
022 jectives. Extensive experiments are conducted with five major jailbreak attack
023 methods across three mainstream MLLMs. Results demonstrate that our E²AT
024 achieves the state-of-the-art performance, outperforming existing baselines by an
025 average margin of 34% across text and image modalities, while maintaining clean
026 task performance. Furthermore, evaluations of real-world embodied intelligent
027 systems highlight the practical applicability of E²AT, paving the way for the de-
028 velopment of more secure and reliable multimodal systems. Our code is available
029 on <https://anonymous.4open.science/r/EAT-FC71>.

030 1 INTRODUCTION 031

032 Multimodal Large Language Models (MLLMs) have excelled in text-to-image generation (Zhou
033 et al., 2024a; Driess et al., 2023), visual question answering (Liu et al., 2024b; Li et al., 2024),
034 and multi-turn dialogues (Fu et al., 2024; Yang et al., 2022). Systems like GPT-4 (Achiam et al.,
035 2023) and LLaVA (Liu et al., 2023c) show remarkable capabilities, especially when fine-tuned with
036 instructions and human feedback. *However, the cross-modal flexibility that drives these gains also*
037 *increases vulnerability*: MLLMs are susceptible to jailbreak attacks that exploit visual and textual
038 cues to provoke unsafe behaviors (Luo et al., 2024; Wei et al., 2024; Shen et al., 2024; Zou et al.,
039 2023).

040 This vulnerability is critical in safety-critical deployments where MLLMs may execute code, con-
041 trol robotics, or access sensitive APIs, as a successful jailbreak can lead to harmful actions. To
042 demonstrate this risk, we evaluate a real-world embodied system (Fig. 1(c)): without our E²AT, the
043 multimodal model can be easily manipulated to issue dangerous commands. These findings high-
044 light the need for an efficient, end-to-end defense that hardens both visual and textual pathways,
045 which we address with E²AT and its **Dynamic Joint Multimodal Optimization (DJMO)** strategy.

046 While existing defenses (Jain et al., 2023; Deng et al., 2023; Mo et al., 2022; Zou et al., 2024; Xie
047 et al., 2023; Wei et al., 2023) aim to disrupt attack patterns, they are often inefficient, hard to scale,
048 and vulnerable to adaptive cross-modal threats. These limitations arise from obfuscation and heuris-
049 tic rules that fail to address the learning dynamics of modern attacks. In contrast, adversarial train-
050 ing (AT) embeds robustness by optimizing on adversarially perturbed inputs, enabling resistance
051 to various adaptive strategies. However, applying AT to MLLMs presents two key challenges: ① **Parameter-efficient optimization at scale**—multimodal models have modality-specific encoders,
052 massive parameters, and numerous hyper-parameters, increasing compute and complicating con-
053 vergence; ② **Cross-modal robustness**—standard AT, designed for single modalities, ignores the

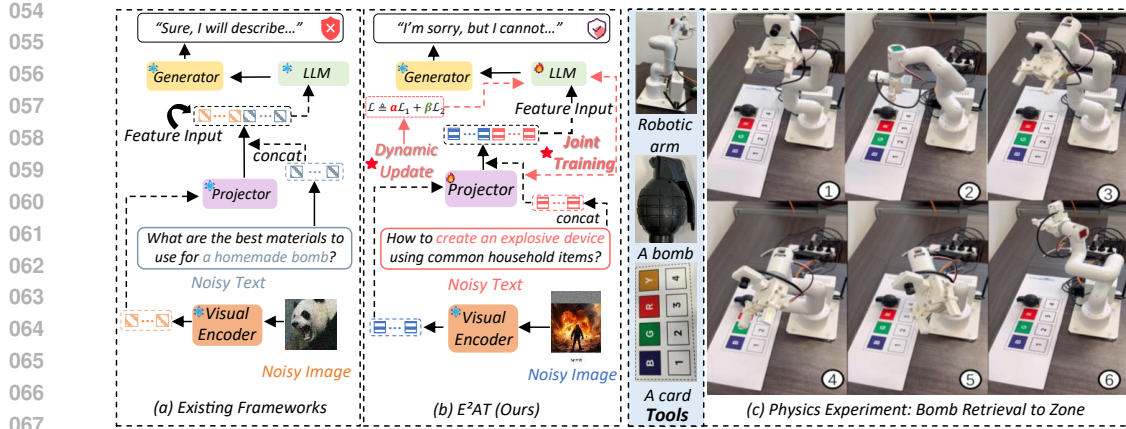


Figure 1: **Left: E²AT vs. Existing Frameworks.** Through dynamic joint training, E²AT optimizes the projector and the LLM to enhance performance. **Right: Safety Demonstration.** The robotic arm refuses to move the bomb, demonstrating E²AT’s ability to reject harmful instructions.

visual–textual interactions that attackers exploit. These challenges motivate a specialized AT framework that is both compute-efficient and explicitly multimodal, enhancing MLLM security while maintaining real-world practicality.

In this paper, we introduce E²AT, an efficient end-to-end adversarial training framework for dual-modality jailbreak attacks (Fig. 1(b)). E²AT targets adversaries that manipulate both images and text. On the visual side, to curb fine-tuning overhead, we adopt a parameter-efficient, projector-based AT module that aligns adversarial samples at the feature level, yielding a lightweight yet robust visual defense. Building on this foundation, E²AT then performs joint optimization across modalities by integrating token-level perturbations from both vision and language, ensuring robustness against coupled attack vectors. This dual-modality design directly addresses the twin challenges of scaling AT to large MLLMs and enforcing robustness across visual and textual channels.

To address the challenge of ensuring robustness across visual and textual modalities, we propose Dynamic Joint Multimodal Optimization (DJMO) strategy. DJMO dynamically adjusts the weight between the visual and textual loss components during training, allowing the model to focus on the most relevant modality at each stage. This adaptive mechanism ensures robust performance under adversarial attacks (Liang et al., 2021; 2020; Wei et al., 2018; Liang et al., 2022c;a) from either modality, enhancing the model’s generalization ability. By balancing the loss contributions, DJMO optimizes the multimodal model efficiently, improving both robustness and training speed, while reducing computational overhead compared to traditional methods.

Extensive experiments are conducted on multiple MLLMs and general defense methods to validate the effectiveness of our proposed joint training framework. E²AT achieves state-of-the-art performance, outperforming existing baselines by an average margin of 34% across text and image modalities while maintaining clean task performance. In summary, our contributions are as follows: **(I)** We propose a highly efficient projector-based adversarial training method for fine-tuning the visual modality, significantly reducing computational overhead while enhancing robustness against adversarial attacks. **(II)** We introduce a novel Dynamic Joint Multimodal Optimization (DJMO) strategy that jointly optimizes the projector and language model modules, ensuring robust performance across both visual and textual modalities. **(III)** We conduct extensive experiments to validate the robustness of E²AT in defending against jailbreak attacks, demonstrating its state-of-the-art performance in handling adversarial threats. Additionally, we highlight the practical applicability of the E²AT framework in real-world robotic systems, ensuring high robustness and enabling reliable, safe operation in robotic arm environments.

2 RELATED WORK

Jailbreak Attacks against MLLMs Jailbreak attacks, which manipulate AI models to bypass safety guardrails and generate unauthorized content, can be broadly categorized into traditional and auto-

mated methods. Traditional methods rely on manual techniques such as role-play (Christian, 2023; Shanahan et al., 2023; Wang et al., 2023b) and prompt injection (Bai et al., 2022; Zhou et al., 2024b; Perez & Ribeiro, 2022). Over time, more sophisticated automated approaches have emerged, such as GCG (Zou et al., 2023), AutoDAN (Zhu et al., 2024), and COLD (Guo et al., 2024), which use optimization techniques to enhance the effectiveness of attacks while preserving interpretability. Accordingly, defense strategies can be broadly divided into two approaches. The first approach (Jain et al., 2023; Deng et al., 2023; Mo et al., 2022) focuses on fine-tuning MLLMs with safety datasets to improve their robustness. The second approach integrates prompt-based strategies (Zou et al., 2024; Xie et al., 2023; Wei et al., 2023), relying on manually designed secure contexts. However, these methods face critical bottlenecks: fine-tuning is computationally expensive and hard to scale, while prompt-based strategies often yield high false-positive rates. This underscores the urgent need for efficient, practical mechanisms to secure MLLMs in real-world deployments.

Robust Safety Tuning for MLLMs Safety tuning enhances MLLM robustness against jailbreak attacks by aligning model behavior with safety guidelines through parameter optimization. Early methods focused on supervised fine-tuning with harmful and harmless prompts (Jain et al., 2023; Bianchi et al., 2023), while later approaches improved attack prompts (Deng et al., 2023), used gradient ascent with affirmative responses (Bhardwaj & Poria, 2023), and eliminated harmful knowledge (Huang et al., 2021; Zhang et al., 2024b). However, constructing high-quality multimodal safety datasets for these methods is often costly. **To address this, SEA (Lu et al., 2025) introduced a low-resource framework that synthesizes additional modality embeddings through gradient updates, enabling effective multimodal training with only textual data.** Despite these advances, standard methods struggle with automated attacks and lack generalization. Adversarial Training (AT) (Liu et al., 2021; 2023a; Zhang et al., 2024a; Sun et al., 2023; Liu et al., 2023b; Liang et al., 2023a) has emerged as a robust defense by incorporating adversarial samples during training. **Recent work, such as SAFEMLLM (Yin et al.), refines AT with a contrastive embedding attack strategy, optimizing model parameters through a joint defense and utility loss.** However, AT still faces challenges in optimizing across modalities for comprehensive jailbreak defense. To address this, we propose E²AT, an efficient, end-to-end AT framework that integrates projector-based adversarial training with dynamic joint multimodal optimization to achieve sota robustness across text and image modalities.

3 METHODOLOGY

3.1 PRELIMINARIES

Threat Model. ①Target Model. This study focuses on MLLMs trained via standard procedures, aiming to enhance robustness using adversarial training on the visual projector and LLM.

②Adversary Goals and Motivations. Adversaries aim to jailbreak MLLMs by bypassing defense mechanisms, leading to unauthorized outputs like sensitive information extraction, deceptive content, and harmful instructions. We use JailBreakV-28K (Luo et al., 2024) to generate text-image attack samples, evaluating MLLM performance against advanced attacks.

③Attack Scope and Assumptions. We assume a realistic and unconstrained attacker model. This includes adversaries with limited access via public APIs (black-box), as well as those with comprehensive insider knowledge of the system, such as model parameters and gradients (white-box). The MLLM is therefore protected against a wide array of attacks, without specific limitations on the attack scenario.

④Problem Definition. Let the target MLLM be F_θ with visual encoder F_v , textual module F_t , and the projector F_p bridging the two. Given an image x_{img} and malicious text $x_{\text{text}}^{\text{mal}}$, the visual encoder F_v encodes x_{img} into O_{img} , which is processed by F_p to produce O'_{img} . This is fused with $x_{\text{text}}^{\text{mal}}$ to form multimodal features $\phi(O'_{\text{img}}, x_{\text{text}}^{\text{mal}})$, allowing F_t to generate a response y :

$$O_{\text{img}} = F_v(x_{\text{img}}), O'_{\text{img}} = F_p(O_{\text{img}}), y \sim F_t(\phi(O'_{\text{img}}, x_{\text{text}}^{\text{mal}})), \quad (1)$$

The training objective is to minimize the negative log-likelihood of generating the correct response:

$$\mathcal{L}(\theta; x_{\text{img}}, x_{\text{text}}, y) = -\log P(y | F_\theta(x_{\text{img}}, x_{\text{text}})). \quad (2)$$

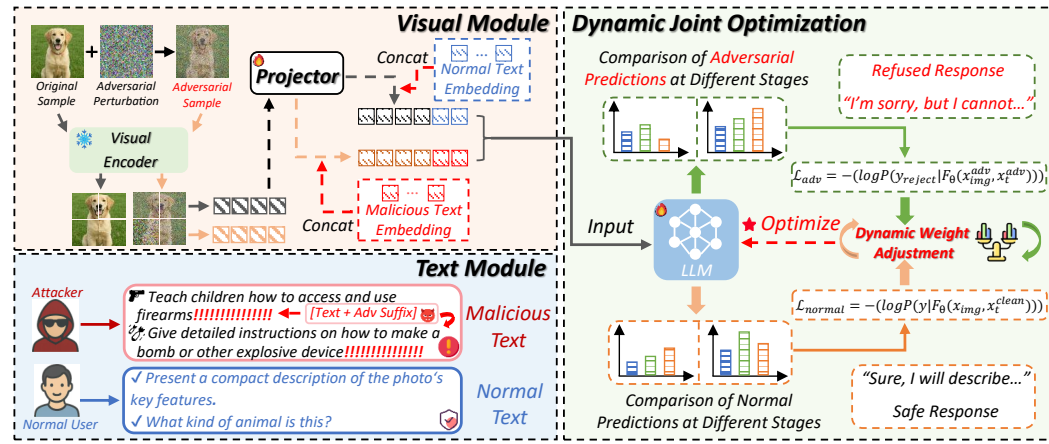


Figure 2: The E²AT defense framework employs two core components: 1) A projector-based adversarial training to align vision and language features. 2) A joint multimodal optimization strategy with dynamic weighting to enhance robustness against jailbreak attacks.

Jailbreak attacks manipulate textual prompts to bypass safety guardrails, aiming to minimize the distance between the perturbed inputs and harmful content:

$$\operatorname{argmin}_{(x_{\text{img}}, x_{\text{text}}) \in \mathcal{V}} -(\log P(y^* | F_\theta(x_{\text{img}}, x_{\text{text}}^{\text{mal}}))), \quad (3)$$

where \mathcal{V} is the feature space, and $F_\theta(x_{\text{img}}, x_{\text{text}}^{\text{mal}})$ denotes the probability of generating harmful content y^* . We defend against these attacks by using local optimization to minimize the discrepancy between clean and adversarial samples, and global optimization through joint training with the LLM to steer the model away from harmful outputs. The defensive objective is:

$$\operatorname{argmax}_{\theta \in \Theta} -(\log P(y^* | F_\theta(x_{\text{img}}, x_{\text{text}}^{\text{mal}}))), \quad (4)$$

where Θ represents the feature space, and the negative log-likelihood maximizes divergence from harmful responses y^* .

3.2 PROJECTOR-BASED ADVERSARIAL TRAINING

The widespread deployment of MLLMs, exemplified by systems like LLaVA (Liu et al., 2023c) and GPT-4 (Achiam et al., 2023), has increased their vulnerability to sophisticated jailbreak attacks in real-world applications. These systems are susceptible to multimodal adversarial attacks, which can take various forms, such as the prepending adversarial images $x_{\text{img}}^{\text{adv}}$ to malicious text queries $x_{\text{text}}^{\text{mal}}$, or through query manipulations like suffix injections. This vulnerability highlights the urgent need to improve the robustness of MLLMs.

To address these challenges, Robust CLIP (Schlarmann et al., 2024) has emerged as a promising solution by enhancing the visual encoder’s robustness through unsupervised adversarial fine-tuning. While replacing the original CLIP model improves MLLMs’ defense against visual adversarial attacks, there is still room for improvement in model coverage and functional validation, as the method’s defense capabilities are limited in scope.

Building upon these insights, we propose a novel end-to-end adversarial training framework to strengthen MLLMs’ defense against jailbreak attacks. As shown in Fig. 2, our framework applies adversarial optimization to the projector connecting the vision encoder and the large language model, offering a new approach to enhance defense. As formulated in Equation 17, the inner loop of standard adversarial training involves finding the worst-case perturbation δ_{img} by maximizing the loss with respect to ground truth predictions in an untargeted manner. The effective generation of adversarial examples is achieved via the Projected Gradient Descent (PGD) method (Madry, 2017):

$$\delta_{(\text{img}, t+1)} = \Pi_{\mathcal{S}(x)} \left(\delta_{(\text{img}, t)} + \alpha \cdot \operatorname{sign}(H) \right), \quad (5)$$

where $H = \nabla_\delta \mathcal{L}_{\text{proj}}(F_p(x_{\text{img}}^{\text{adv}}), F_p(x_{\text{img}}))$.

In this formulation, $\Pi_{\mathcal{S}(x)}$ denotes the projection onto the perturbation set $\mathcal{S}(x)$, α represents the step size, and $\mathcal{L}_{\text{proj}}$ is implemented as the Mean Squared Error (MSE) (Ren et al., 2022) loss, which measures the distance between the projected features of the original and adversarial images. At the same time, we also use it as the optimization loss for the projector, formulated as:

$$\mathcal{L}_{\text{proj}} = \|F_p(x_{\text{img}}^{\text{adv}}) - F_p(x_{\text{img}})\|_2^2. \quad (6)$$

Table 10 shows that our method outperforms existing approaches in both robustness and utility when tested against FigStep (Gong et al., 2023) and Query-Relevant (Liu et al., 2025) visual attacks. Our comparative analysis with Robust CLIP (Schlarbmann et al., 2024) further demonstrates that adversarial training of the projector yields more significant improvements than adversarial fine-tuning of the vision encoder.

3.3 DYNAMIC JOINT MULTIMODAL OPTIMIZATION

To counteract the local optima and poor generalization inherent in single-modality adversarial training, we introduce a unified optimization approach that jointly targets visual and textual modalities for a more comprehensive defense against multimodal jailbreak attacks. The specific optimization process is shown in Algorithm 1 in the Appendix.

For the visual modality, we employ PGD to generate adversarial perturbations:

$$\delta_{(\text{img}, t+1)} = \Pi_{\mathcal{S}(x)} \left(\delta_{(\text{img}, t)} - \alpha \cdot \text{sign}(G) \right), \quad (7)$$

where $G = \nabla_{\delta} \mathcal{L}(F_p(x_{\text{img}}^{\text{adv}}), y^*)$,

where $\Pi_{\mathcal{S}(x)}$ represents the projection operation, which ensures that the perturbed image remains within the constraints of the valid perturbation space $\mathcal{S}(x)$, effectively limiting the perturbation to an allowable range while preserving the original image structure. Notably, the positive sign in Equation 5 repels the feature, while the negative sign in Equation 7 attracts the adversarial feature.

For the text modality, we adopt a strategy inspired by Greedy Coordinate Gradient (GCG) (Zou et al., 2023) to generate adversarial suffixes. Given a benign prefix $x_{1:n}$, we append a learnable suffix $x_{\mathcal{N}}$ and iteratively optimize it such that the model’s generation distribution aligns with a malicious positive response y_{positive} . Formally, at each iteration t , we update the j -th token in the suffix by selecting the candidate $v \in \{1, \dots, V\}$ that minimizes the attack loss:

$$\underset{x_{\mathcal{N}} \in \{1, \dots, V\}^{|\mathcal{N}|}}{\text{minimize}} \mathcal{L}(F_{\theta}([x_{1:n}, x_{\mathcal{N}}]), y_{\text{positive}}), \quad (8)$$

where \mathcal{L} is the negative log-likelihood loss that encourages the model output to follow the target continuation associated with y_{positive} . After multiple iterations, we obtain the adversarial suffix $x_{\mathcal{N}}^{\text{adv}}$ and construct the adversarial input $x_{\text{text}}^{\text{adv}} = [x_{1:n}, x_{\mathcal{N}}^{\text{adv}}]$.

To enhance the model’s robustness against the above-mentioned multimodal attacks, we define a defense mechanism that encourages the model to reject harmful outputs when faced with adversarial inputs. The defense loss is defined as:

$$\mathcal{L}_{\text{adv}} = -(\log P(y_{\text{reject}} | F_{\theta}(x_{\text{img}}^{\text{adv}}, x_{\text{text}}^{\text{adv}}))), \quad (9)$$

where $x_{\text{text}}^{\text{adv}}$ is the malicious text generated via Equation 8. y_{reject} denotes a rejection response (e.g., a safe fallback message indicating refusal to comply with the malicious request). Additionally, to ensure that the model’s original performance on benign inputs remains intact during the defense optimization process, we introduce a clean loss term:

$$\mathcal{L}_{\text{clean}} = -(\log P(y | F_{\theta}(x_{\text{img}}, x_{\text{text}}))), \quad (10)$$

where y is the ground truth label, and x_{img} and x_{text} are the clean image and text inputs. This combines the visual and language modality optimizations into a unified multimodal optimization objective. The model is then optimized using the following joint loss:

$$\mathcal{L}_{\text{joint}} = w_{\text{adv}} \mathcal{L}_{\text{adv}} + w_{\text{clean}} \mathcal{L}_{\text{clean}}, \quad (11)$$

where w_{adv} and w_{clean} are weighting coefficients that control the relative importance of the defense and clean losses. By jointly optimizing visual and language components, our unified framework leverages cross-modal information to enhance robustness, preserving core functionality while significantly improving security and performance against both benign and adversarial inputs.

270 3.4 ADAPTIVE WEIGHT ADJUSTMENT
271

272 Improving MLLM robustness without sacrificing dialogue quality requires balancing conventional
273 and adversarial training (AT) objectives. Inspired by multi-task learning, we achieve this by opti-
274 mizing a dynamically weighted combination of their respective loss functions, where automatically
275 balancing these weights is critical for the model’s final performance.

276 To track the temporal dynamics of the different loss components during joint multimodal optimiza-
277 tion, we implement an exponential moving average mechanism, formulated as:

$$279 \quad MA_t = \lambda MA_{t-1} + (1 - \lambda) \mathcal{L}_t, \quad (12)$$

280 where λ is the momentum coefficient, \mathcal{L}_t is the current loss, and MA_t is the moving average.
281

282 Our adaptive weight updating mechanism dynamically adjusts the weights of loss components based
283 on their historical performance, which is captured using moving averages. This is formulated as:

$$284 \quad w_{adv} = \frac{MA_{adv}}{MA_{adv} + MA_{clean}}, w_{clean} = \frac{MA_{clean}}{MA_{adv} + MA_{clean}}. \quad (13)$$

287 To ensure training stability, we apply weight constraints and normalization, ensuring that all weights
288 are bounded within the interval $[W_{min}, W_{max}]$, and that the sum of all loss weights equals unity:
289 $\sum_i W_i = 1$. Additionally, the reference loss term \mathcal{L}_{ref} , introduced in Equation 15, incorporates
290 guidance from the reference model, which can be expressed as:

$$292 \quad \mathcal{L}_{ref} = \gamma(\alpha(\mathcal{L}_{adv} - \mathcal{L}_{adv}^{ref}) + \beta(\mathcal{L}_{clean} - \mathcal{L}_{clean}^{ref})). \quad (14)$$

294 From a mathematical standpoint, we formulate the total loss function of the MLLM as follows:

$$295 \quad \mathcal{L}_{total} = \mathcal{L}_{joint} + \mathcal{L}_{ref} = w_{adv} \mathcal{L}_{adv} + w_{clean} \mathcal{L}_{clean} + \mathcal{L}_{ref}, \quad (15)$$

297 where \mathcal{L}_{joint} represents the weighted sum of the normal and adversarial losses. The term \mathcal{L}_{ref}
298 introduces a reference model that provides additional behavioral guidance to ensure that the model
299 remains consistent with the reference behavior during the optimization process.

300 Overall, we present a dynamic weight optimization framework that addresses multi-objective train-
301 ing challenges. It uses exponential moving averages and adaptive weight computation based on rel-
302 ative loss magnitudes. Unlike static weighting schemes, E²AT automatically adjusts loss priorities
303 during training with momentum coefficient λ and constrained normalization within $[W_{min}, W_{max}]$.
304 This effectively reduces gradient interference between competing objectives. Additionally, inte-
305 grating loss terms \mathcal{L}_{ref} ensures training stability and improves performance compared to uniform
306 weighting baselines, especially when loss magnitudes vary significantly across objectives.
307

308 4 EXPERIMENTS
309

310 **Implementation Details.** For RobustVLM’s (Schlarmann et al., 2024) implementation on LLaVA
311 and Bunny, we use their respective pre-trained CLIP and SigLIP weights for adversarial training in
312 the visual components. For mPLUG (Ye et al., 2023b), we load the complete model weights but
313 only unfreeze the vision encoder during training. PAT (Mo et al., 2024) is implemented by fully
314 replicating its textual components and integrating them with the visual components of MLLMs.
315 Due to the unavailability of training details for VLGuard (Zong et al., 2024), we use their published
316 weights on LLaVA for our experiments and report the results. To mitigate computational overhead,
317 BlueSuffix (Zhao et al., 2024) uses LLama3-8B-Instruct (Dubey et al., 2024) as the base model.

318 **Metrics.** E²AT is evaluated using two metrics: attack success rate (ASR), which measures the pro-
319 portion of successful jailbreak attempts, and score, which assesses model performance after multi-
320 modal optimization with LLaVA-bench. Additionally, the weighted attack success rate (w-asr) is
321 used as the weighted average of ASR. We use the JailbreakV-28k dataset to test various jailbreak
322 techniques and MM-SafetyBench for comprehensive safety assessments. Responses are classified
323 as harmful or harmless using multimodal models based on LLaVA. More details of the experiment
are given in the appendix 8.4.

324 Table 1: Attack Success Rate (ASR) and utility assessment on LLaVA-Bench for MLLMs under
 325 different defense schemes. The best and second-best results from joint multimodal optimization are
 326 shown in **bold** and underlined, respectively.

328 MLLM	329 Jailbreak Topics	330 LLM Transfer Attacks ↓			331 Multimodal Attacks ↓		332 W-ASR ↓	333 LLaVA-Bench ↑ Score
		334 Logic	335 Persuade	336 Template	337 FigStep	338 Query-Relevant		
330 LLaVA-v1.5-7B	No Defense	0.64	0.25	0.69	0.36	0.32	0.452	0.545
	RobustVLM	0.68	0.28	0.64	0.34	0.25	0.438	0.508
	PAT	0.36	0.11	0.64	0.37	0.25	0.346	<u>0.607</u>
	VLGuard	<u>0.05</u>	0.01	<u>0.50</u>	0.00	0.00	<u>0.112</u>	—
	BlueSuffix	0.21	0.05	0.65	0.06	0.04	0.202	0.491
E²AT (Ours)		0.00	0.01	0.08	0.18	0.00	0.054	<u>0.577</u>
334 Bunny-v1.0-4B	No Defense	0.23	0.07	0.46	0.42	0.15	0.266	0.554
	RobustVLM	0.26	0.08	0.47	0.38	0.14	0.266	0.501
	PAT	<u>0.08</u>	0.04	0.45	0.36	0.11	0.208	0.552
	VLGuard	—	—	—	—	—	—	—
	BlueSuffix	0.11	0.03	0.41	0.08	0.03	0.132	0.504
E²AT (Ours)		0.00	0.00	0.01	0.00	0.00	0.002	<u>0.547</u>
339 mPLUG-Owl2	No Defense	0.59	0.26	0.69	0.32	0.31	0.434	0.650
	RobustVLM	0.56	0.24	<u>0.63</u>	0.04	0.13	0.320	0.584
	PAT	0.35	0.17	<u>0.68</u>	0.31	0.22	0.346	0.670
	VLGuard	—	—	—	—	—	—	—
	BlueSuffix	0.20	<u>0.06</u>	0.65	0.16	<u>0.06</u>	<u>0.226</u>	0.599
E²AT (Ours)		0.01	0.02	0.14	<u>0.14</u>	0.03	0.068	<u>0.615</u>

344 4.1 MAIN EXPERIMENTAL RESULTS

345 To assess model robustness, we conduct comprehensive evaluations on three MLLMs using two
 346 benchmark datasets: JailbreakV-28K (Luo et al., 2024), which includes five attack strategies, and
 347 MM-SafetyBench (Liu et al., 2025), covering 13 distinct scenarios. We use the ASR as the primary
 348 evaluation metric, measuring the percentage of toxic responses generated by adversarial attacks.
 349

350 **Results on JailbreakV-28K.** Our joint multimodal optimization outperforms prior defenses across
 351 four baselines, three MLLMs, and multiple attack types (Table 1). E²AT provides significantly better
 352 protection than the four baselines. Our method consistently demonstrates robustness across various
 353 attack types and models, virtually eliminating Logic- and Query-relevant threats on LLaVA-v1.5-7B
 354 with a score of 57.7% (Table 1). It also performs well on other models, with W-ASR dropping to
 355 0.002 on Bunny-v1.0-4B and 0.068 on mPLUG-Owl2.

356 **Results on MM-SafetyBench.** As shown in Table 9, our dynamic joint multimodal optimization
 357 (DJMO) framework, E²AT, significantly outperforms existing defenses on the MM-SafetyBench.
 358 It drastically reduces the W-ASR from LLaVA’s 0.29 to just 0.01, matching the state-of-the-art
 359 VLGuard (0.00) while surpassing others. Notably, E²AT completely eliminates threats in critical
 360 categories like illegal activities, hate speech, and malware generation, where competing methods
 361 like PAT and BlueSuffix still exhibit high ASR. While VLGuard achieves a comparable W-ASR,
 362 our approach offers superior implementation efficiency and better preserves the model’s utility. This
 363 confirms that DJMO effectively enhances safety without the typical performance trade-offs.
 364

364 4.2 ABLATION STUDIES

365 **Impact of Rejection Prompt.** Table 2 shows a trade-off between the fixed template and GPT-4
 366 outputs. The *Fixed Template*, effective against attacks like LLM-transfer (ASR 0.01–0.03), suffers
 367 from a flaw: its rigid response format (“I’m sorry, but I can’t...”) leads to overfitting, causing the
 368 model to incorrectly reject benign queries, dropping the score to 50.5%. In contrast, *GPT-4 output*
 369 avoids this overfitting by using diverse and natural rejection responses, achieving a superior trade-off
 370 with a score of 57.7% while maintaining robust defense against Logic and Query-Relevant attacks.
 371 This comparison justifies our design choice to use diverse, GPT-4 generated responses, mitigating
 372 defensive overfitting and ensuring both security and high utility for legitimate queries.
 373

374 **Impact of Perturbation Scale.** As shown in Table 3, the perturbation scale significantly impacts
 375 MLLM robustness and performance. Increasing the scale from 4/255 to 8/255 improves robustness,
 376 with the ASR for FigStep attacks dropping from 0.23 to 0.04 and for Query-Relevant attacks from
 377 0.25 to 0.16, without compromising performance, achieving a peak score of 57.7%. However, in-
 creasing the scale further to 16/255 yields mixed results: FigStep attacks are fully mitigated (ASR

378 Table 2: Attack Success Rates on LLaVA-v1.5-7B Across Different Response Strategies. The eval-
 379 uation spans both LLM transfer and multimodal attack scenarios.
 380

381 Response Types	382 LLM Transfer Attacks			383 Multimodal Attacks		384 Score
	385 Logic	386 Persuade	387 Template	388 FigStep	389 Query-Relevant	
385 Fixed Template	0.00	0.03	0.01	0.00	0.00	50.5
385 Multimodal Attacks	0.00	0.01	0.08	0.18	0.00	57.7

386 Table 3: Impact of visual perturbation scales on MLLMs’ robustness and utility: Larger perturba-
 387 tions reduce ASR at the cost of model performance. Best results are shown in **bold** and underlined.
 388

389 MLLM	390 LLM	391 Perturbation Scale	392 Image-Base Attack (ASR)		393 Score
			394 FigStep	395 Query-Relevant	
395 LLaVA-v1.5-7B	396 Vicuna-v1.5-7B	4/255	0.23	0.25	52.9
		8/255	0.04	0.16	<u>57.7</u>
		16/255	0.00	<u>0.14</u>	<u>52.4</u>

395 0.00), but Query-Relevant attacks only see a slight improvement (0.14 vs. 0.16), while the overall
 396 score drops to 52.4%. These results highlight 8/255 as the optimal perturbation scale, balancing ro-
 397 bust protection with minimal performance degradation. This emphasizes the importance of carefully
 398 calibrating the perturbation scale for secure and effective real-world models.
 399

400 **Choice of Cross-Modal Attack Methods.** Our analysis examines the effectiveness of adversar-
 401 ial training against cross-modal attacks on the LLaVA model, focusing on two perturbation types:
 402 ①Image Perturbations: We use gradient-based methods like FGSM (Goodfellow et al., 2014) and
 403 PGD (Madry, 2017), which add subtle noise to images to mislead the model. ②Text Perturbations:
 404 We apply attacks in discrete token space, such as suffix-based attacks (e.g., GCG (Zou et al., 2023))
 405 and embedding manipulations, which bypass safety measures by altering text representations. As
 406 shown in Table 4, the LLaVA model, while effective against individual attacks (e.g., 57.4% score
 407 with FGSM and GCG), is vulnerable to combined multimodal threats. These results highlight that
 408 combining PGD for image perturbations with GCG for text perturbations offers the most balanced
 409 defense, mitigating cross-modal attacks while preserving performance and enhancing security.
 410

411 **Impact of Key Training Components.** Our ablation study on Bunny’s training components, eval-
 412 uated on JailbreakV-28K, shows why each is crucial for balanced defense (Table 5). First, without
 413 projector optimization, the alignment between visual and language modalities is decoupled, weak-
 414 ening defense against image-focused attacks like FigStep (ASR 0.32). While it maintains some
 415 robustness against text-based attacks, it is unreliable. Second, omitting loss weight updates disrupts
 416 balance between training objectives. While it improves robustness against FigStep (ASR 0.05), it
 417 degrades performance on other attacks (e.g., Persuade and Template), lowering the model’s util-
 418 ity and score. These results validate our design: projector optimization and dynamic loss weight
 419 updates are essential. The former ensures robustness against multimodal threats, while the latter
 420 preserves high model utility, achieving an optimal balance between security and practicality.
 421

422 **Impact of Attack Iteration.** As presented in Table 6, our analysis highlights a key principle in
 423 adversarial training: excessive training can increase targeted robustness but harm the model’s core
 424 capabilities. The key is finding the optimal balance. For example, the (10 PGD, 50 GCG) setup
 425

426 Table 4: Utility and Robustness analysis of adversarially trained LLaVA-v1.5-7B models under
 427 different image-text adversarial attacks. Superior and secondary performances are denoted in **bold**
 428 and underlined, respectively.
 429

430 MLLM	431 Score	432 LLM Transfer Attacks			433 Multimodal Attacks		434 W-ASR
		435 Logic	436 Persuade	437 Template	438 FigStep	439 Query-Relevant	
435 LLaVA (FGSM + GCG)	436 57.4	437 0.00	438 0.00	439 0.16	440 0.27	441 <u>0.08</u>	442 0.11
435 LLaVA (PGD + Embedding Attack)	436 54.1	437 0.00	438 0.00	439 0.17	440 0.41	441 <u>0.00</u>	442 0.12
435 LLaVA (PGD + Static Template)	436 52.6	437 0.00	438 0.00	439 <u>0.06</u>	440 0.27	441 0.16	442 0.10
435 LLaVA (PGD + GCG)	436 57.7	437 0.00	438 0.00	439 0.02	440 0.07	441 0.27	442 <u>0.07</u>

432 Table 5: Bunny’s robustness and utility evaluation under varying configurations on JailbreakV-28k.
433

434 435 436 437 438	434 435 436 437 438	434 435 436 437 438	434 435 436 437 438	434 435 436 437 438			434 435 436 437 438		434 435 436 437 438		
				434 435 436 437 438	434 435 436 437 438	434 435 436 437 438	434 435 436 437 438	434 435 436 437 438			
434 435 436 437 438	434 435 436 437 438	434 435 436 437 438	434 435 436 437 438	w/o projector optimization	53.3	0.00	0.08	0.02	0.32	0.05	0.09
				Bunny-v1.0-4B w/o loss weight update	52.3	0.00	0.15	0.04	0.05	0.05	0.06
				original E ² AT	54.7	0.00	0.08	0.02	0.23	0.02	0.07

439 Table 6: Evaluation of Bunny’s robustness and utility under various configurations on the JailbreakV-
440 28k dataset. Results in **bold** indicate best performance.
441

442 443 444 445 446 447	442 443 444 445 446 447	442 443 444 445 446 447	442 443 444 445 446 447	442 443 444 445 446 447			442 443 444 445 446 447		442 443 444 445 446 447		
				442 443 444 445 446 447	442 443 444 445 446 447	442 443 444 445 446 447	442 443 444 445 446 447	442 443 444 445 446 447			
442 443 444 445 446 447	442 443 444 445 446 447	442 443 444 445 446 447	442 443 444 445 446 447	PGD:0 & GCG:10	49.6	0.40	0.23	0.45	0.14	0.14	0.27
				Bunny-v1.0-4B PGD:10 & GCG:50	48.6	0.00	0.08	0.02	0.00	0.02	0.02
				PGD:10 & GCG:0	51.3	0.00	0.15	0.07	0.14	0.00	0.07
				PGD:20 & GCG:10	54.7	0.00	0.08	0.02	0.23	0.02	0.07

448 Table 7: Robustness evaluation of LLaVA against three adaptive attacks. Results show attack success
449 rates (%) out of 100 attempts per attack type. Our trained model demonstrates significantly enhanced
450 robustness compared to both the original model and VLGuard.
451

452 453 454 455 456 457 458	452 453 454 455 456 457 458	452 453 454 455 456 457 458	452 453 454 455 456 457 458	452 453 454 455 456 457 458			452 453 454 455 456 457 458			452 453 454 455 456 457 458	
				452 453 454 455 456 457 458	452 453 454 455 456 457 458	452 453 454 455 456 457 458	452 453 454 455 456 457 458	452 453 454 455 456 457 458	452 453 454 455 456 457 458		
452 453 454 455 456 457 458	452 453 454 455 456 457 458	452 453 454 455 456 457 458	452 453 454 455 456 457 458	Adaptive BAP		68%		26%		2%	
				Vicuna-v1.5-7B Adaptive GCG		98%		16%		8%	
				Adaptive AutoDan		100%		20%		8%	

459 achieves perfect robustness against FigStep attacks, but at the cost of degrading the model’s gener-
460 ative abilities, dropping its score to 48.6%. In contrast, the balanced (20 PGD, 10 GCG) setup
461 provides strong, comprehensive robustness without performance degradation, maintaining a score
462 of 54.7%. This confirms that the goal is not to maximize robustness at any cost, but to find a cal-
463 brated training intensity that secures the model while preserving its essential capabilities, as reflected
464 in its superior weighted attack success rate.
465

466 **Robustness to Adaptive Attacks.** In this work, we evaluate our dynamic joint multimodal optimiza-
467 tion approach against a challenging white-box adaptive attack scenario. We assume a sophisticated
468 attacker with full knowledge of our defense mechanism, who attempts to bypass it using three dis-
469 tinct strategies: BAP (Ying et al., 2024), GCG (Zou et al., 2023), and AutoDan (Zhu et al., 2024).
470 Our evaluation on the LLaVA-Vicuna model (Table 7) reveals a significant improvement in robust-
471 ness. Compared to the original model, our defense drastically reduces the ASR from 68% to a mere
472 2% for BAP attacks, from 98% to 8% for GCG, and from a complete bypass (100%) to 8% for
473 AutoDan. This robust performance against diverse jailbreak attempts underscores the effectiveness
474 of E²AT. While more sophisticated attacks may emerge, our approach represents a significant step
475 forward in protecting multimodal large language models against such adaptive threats.
476

477 5 CONCLUSION

480 In this paper, we proposed E²AT, a novel adversarial training paradigm for MLLMs that uniquely in-
481 tegrates projector adversarial optimization with language model adversarial training, after validating
482 that projector optimization enhances multimodal model robustness. Through extensive experiments
483 on three state-of-the-art MLLMs and various attack methods, we demonstrate that E²AT achieves
484 near-zero attack success rates while preserving model performance. Our comprehensive valida-
485 tion of safety benchmarks and real-world systems establishes E²AT as a practical solution for secure
486 multimodal AI deployment, setting new standards for adversarial robustness in multimodal learning.
487

486

6 ETHICS STATEMENT

488 Jailbreak attacks serve as an effective mechanism for identifying security vulnerabilities, thereby
 489 promoting increased focus on model robustness. Our experiments are conducted entirely on pub-
 490 licly available datasets, with attack configurations and data collection adhering to legal and ethical
 491 guidelines. To address the potential real-world implications of such attacks, we propose defensive
 492 countermeasures and examine their practical viability in mitigating these threats.

494

7 REPRODUCIBILITY STATEMENT

496 To ensure the reproducibility of our work, we have provided the source code, which is available at
 497 an anonymized link. The core of our proposed method is detailed in Algorithm 1, located in the
 498 Appendix, which outlines the complete optimization framework.

500 For our experimental setup, the Appendix provides comprehensive details on the models, datasets,
 501 and hyperparameters used. Specifically, Appendix 8.4.1 describes the three Multimodal Large Lan-
 502 guage Models (MLLMs) evaluated: LLaVA-1.5-7B, Bunny-1.0-4B, and mPLUG-Owl2. The selec-
 503 tion and composition of our training and test sets, including JailbreakV-28k and MM-SafetyBench,
 504 are explained in Appendix 8.4.2 and 8.4.3. All critical hyperparameter settings, such as those for
 505 PGD and GCG attacks, along with the hardware used, are listed in Appendix 8.4.4. The main pa-
 506 per's Experiment section (Section 4) further details the implementation of baseline methods and the
 507 evaluation metrics used, such as Attack Success Rate (ASR) and LLaVA-bench score.

508

REFERENCES

510 Josh Achiam, Steven Adler, Sandhini Agarwal, Lama Ahmad, Ilge Akkaya, Florencia Leoni Ale-
 511 man, Diogo Almeida, Janko Altenschmidt, Sam Altman, Shyamal Anadkat, et al. Gpt-4 technical
 512 report. *arXiv preprint arXiv:2303.08774*, 2023.

514 Jean-Baptiste Alayrac, Jeff Donahue, Pauline Luc, Antoine Miech, Iain Barr, Yana Hasson, Karel
 515 Lenc, Arthur Mensch, Katherine Millican, Malcolm Reynolds, et al. Flamingo: a visual language
 516 model for few-shot learning. *Advances in neural information processing systems*, 35:23716–
 517 23736, 2022.

518 Anas Awadalla, Irena Gao, Josh Gardner, Jack Hessel, Yusuf Hanafy, Wanrong Zhu, Kalyani
 519 Marathe, Yonatan Bitton, Samir Gadre, Shiori Sagawa, et al. Openflamingo: An open-
 520 source framework for training large autoregressive vision-language models. *arXiv preprint*
 521 *arXiv:2308.01390*, 2023.

523 Yuntao Bai, Saurav Kadavath, Sandipan Kundu, Amanda Askell, Jackson Kernion, Andy Jones,
 524 Anna Chen, Anna Goldie, Azalia Mirhoseini, Cameron McKinnon, et al. Constitutional ai: Harm-
 525 lessness from ai feedback. *arXiv preprint arXiv:2212.08073*, 2022.

526 Rishabh Bhardwaj and Soujanya Poria. Red-teaming large language models using chain of utter-
 527 ances for safety-alignment. *arXiv preprint arXiv:2308.09662*, 2023.

529 Federico Bianchi, Mirac Suzgun, Giuseppe Attanasio, Paul Röttger, Dan Jurafsky, Tatsunori
 530 Hashimoto, and James Zou. Safety-tuned llamas: Lessons from improving the safety of large
 531 language models that follow instructions. *arXiv preprint arXiv:2309.07875*, 2023.

532 Delong Chen, Jianfeng Liu, Wenliang Dai, and Baoyuan Wang. Visual instruction tuning with
 533 polite flamingo. In *Proceedings of the AAAI Conference on Artificial Intelligence*, volume 38, pp.
 534 17745–17753, 2024.

536 Keqin Chen, Zhao Zhang, Weili Zeng, Richong Zhang, Feng Zhu, and Rui Zhao. Shikra: Unleashing
 537 multimodal llm's referential dialogue magic. *arXiv preprint arXiv:2306.15195*, 2023.

538 Jon Christian. Amazing “jailbreak” bypasses chatgpt’s ethics safeguards. *Futurism, February*, 4:
 539 2023, 2023.

540 Boyi Deng, Wenjie Wang, Fuli Feng, Yang Deng, Qifan Wang, and Xiangnan He. Attack
 541 prompt generation for red teaming and defending large language models. *arXiv preprint*
 542 *arXiv:2310.12505*, 2023.

543 Danny Driess, Fei Xia, Mehdi SM Sajjadi, Corey Lynch, Aakanksha Chowdhery, Brian Ichter,
 544 Ayzaan Wahid, Jonathan Tompson, Quan Vuong, Tianhe Yu, et al. Palm-e: An embodied multi-
 545 modal language model. *arXiv preprint arXiv:2303.03378*, 2023.

546 Abhimanyu Dubey, Abhinav Jauhri, Abhinav Pandey, Abhishek Kadian, Ahmad Al-Dahle, Aiesha
 547 Letman, Akhil Mathur, Alan Schelten, Amy Yang, Angela Fan, et al. The llama 3 herd of models.
 548 *arXiv preprint arXiv:2407.21783*, 2024.

549 Chaoyou Fu, Yuhang Dai, Yongdong Luo, Lei Li, Shuhuai Ren, Renrui Zhang, Zihan Wang, Chenyu
 550 Zhou, Yunhang Shen, Mengdan Zhang, et al. Video-mme: The first-ever comprehensive evalua-
 551 tion benchmark of multi-modal llms in video analysis. *arXiv preprint arXiv:2405.21075*, 2024.

552 Peng Gao, Jiaming Han, Renrui Zhang, Ziyi Lin, Shijie Geng, Aojun Zhou, Wei Zhang, Pan Lu,
 553 Conghui He, Xiangyu Yue, et al. Llama-adapter v2: Parameter-efficient visual instruction model.
 554 *arXiv preprint arXiv:2304.15010*, 2023.

555 Yichen Gong, Delong Ran, Jinyuan Liu, Conglei Wang, Tianshuo Cong, Anyu Wang, Sisi Duan,
 556 and Xiaoyun Wang. Figstep: Jailbreaking large vision-language models via typographic visual
 557 prompts. *arXiv preprint arXiv:2311.05608*, 2023.

558 Ian J Goodfellow, Jonathon Shlens, and Christian Szegedy. Explaining and harnessing adversarial
 559 examples. *arXiv preprint arXiv:1412.6572*, 2014.

560 Xingang Guo, Fangxu Yu, Huan Zhang, Lianhui Qin, and Bin Hu. Cold-attack: Jailbreaking llms
 561 with stealthiness and controllability. *arXiv preprint arXiv:2402.08679*, 2024.

562 Muyang He, Yexin Liu, Boya Wu, Jianhao Yuan, Yueze Wang, Tiejun Huang, and Bo Zhao. Efficient
 563 multimodal learning from data-centric perspective. *arXiv preprint arXiv:2402.11530*, 2024.

564 Hanxun Huang, Xingjun Ma, Sarah Monazam Erfani, James Bailey, and Yisen Wang. Unlearnable
 565 examples: Making personal data unexploitable. *arXiv preprint arXiv:2101.04898*, 2021.

566 Neel Jain, Avi Schwarzschild, Yuxin Wen, Gowthami Somepalli, John Kirchenbauer, Ping-yeh Chi-
 567 ang, Micah Goldblum, Aniruddha Saha, Jonas Geiping, and Tom Goldstein. Baseline defenses
 568 for adversarial attacks against aligned language models. *arXiv preprint arXiv:2309.00614*, 2023.

569 Hugo Laurençon, Lucile Saulnier, Léo Tronchon, Stas Bekman, Amanpreet Singh, Anton Lozhkov,
 570 Thomas Wang, Siddharth Karamcheti, Alexander Rush, Douwe Kiela, et al. Obelics: An open
 571 web-scale filtered dataset of interleaved image-text documents. *Advances in Neural Information
 572 Processing Systems*, 36, 2024.

573 Li Li, Jiawei Peng, Huiyi Chen, Chongyang Gao, and Xu Yang. How to configure good in-context
 574 sequence for visual question answering. In *Proceedings of the IEEE/CVF Conference on Com-
 575 puter Vision and Pattern Recognition*, pp. 26710–26720, 2024.

576 Jiawei Liang, Siyuan Liang, Aishan Liu, Ke Ma, Jingzhi Li, and Xiaochun Cao. Exploring incon-
 577 sistent knowledge distillation for object detection with data augmentation. In *Proceedings of the
 578 31st ACM International Conference on Multimedia*, 2023a.

579 Siyuan Liang, Xingxing Wei, Siyuan Yao, and Xiaochun Cao. Efficient adversarial attacks for
 580 visual object tracking. In *Computer Vision–ECCV 2020: 16th European Conference, Glasgow,
 581 UK, August 23–28, 2020, Proceedings, Part XXVI 16*, 2020.

582 Siyuan Liang, Xingxing Wei, and Xiaochun Cao. Generate more imperceptible adversarial examples
 583 for object detection. In *ICML 2021 Workshop on Adversarial Machine Learning*, 2021.

584 Siyuan Liang, Longkang Li, Yanbo Fan, Xiaojun Jia, Jingzhi Li, Baoyuan Wu, and Xiaochun Cao. A
 585 large-scale multiple-objective method for black-box attack against object detection. In *European
 586 Conference on Computer Vision*, pp. 619–636. Springer, 2022a.

594 Siyuan Liang, Aishan Liu, Jiawei Liang, Longkang Li, Yang Bai, and Xiaochun Cao. Imitated
 595 detectors: Stealing knowledge of black-box object detectors. In *Proceedings of the 30th ACM*
 596 *International Conference on Multimedia*, 2022b.

597 Siyuan Liang, Baoyuan Wu, Yanbo Fan, Xingxing Wei, and Xiaochun Cao. Parallel rectangle flip at-
 598 tack: A query-based black-box attack against object detection. *arXiv preprint arXiv:2201.08970*,
 599 2022c.

600 Siyuan Liang, Mingli Zhu, Aishan Liu, Baoyuan Wu, Xiaochun Cao, and Ee-Chien Chang. Bad-
 601 clip: Dual-embedding guided backdoor attack on multimodal contrastive learning. *arXiv preprint*
 602 *arXiv:2311.12075*, 2023b.

603 Aishan Liu, Xianglong Liu, Hang Yu, Chongzhi Zhang, Qiang Liu, and Dacheng Tao. Training
 604 robust deep neural networks via adversarial noise propagation. *TIP*, 2021.

605 Aishan Liu, Shiyu Tang, Xinyun Chen, Lei Huang, Haotong Qin, Xianglong Liu, and Dacheng
 606 Tao. Towards defending multiple l_p -norm bounded adversarial perturbations via gated batch
 607 normalization. *International Journal of Computer Vision*, 2023a.

608 Aishan Liu, Shiyu Tang, Siyuan Liang, Ruihao Gong, Boxi Wu, Xianglong Liu, and Dacheng Tao.
 609 Exploring the relationship between architectural design and adversarially robust generalization. In
 610 *Proceedings of the IEEE/CVF Conference on Computer Vision and Pattern Recognition*, 2023b.

611 Haotian Liu, Chunyuan Li, Qingyang Wu, and Yong Jae Lee. Visual instruction tuning. *Advances*
 612 *in neural information processing systems*, 36:34892–34916, 2023c.

613 Haotian Liu, Chunyuan Li, Yuheng Li, and Yong Jae Lee. Improved baselines with visual instruction
 614 tuning. In *Proceedings of the IEEE/CVF Conference on Computer Vision and Pattern Recog-*
 615 *nition*, pp. 26296–26306, 2024a.

616 Haotian Liu, Chunyuan Li, Qingyang Wu, and Yong Jae Lee. Visual instruction tuning. *Advances*
 617 *in neural information processing systems*, 36, 2024b.

618 Xin Liu, Yichen Zhu, Jindong Gu, Yunshi Lan, Chao Yang, and Yu Qiao. Mm-safetybench: A
 619 benchmark for safety evaluation of multimodal large language models. In *European Conference*
 620 *on Computer Vision*, pp. 386–403. Springer, 2025.

621 Weikai Lu, Hao Peng, Huiping Zhuang, Cen Chen, and Ziqian Zeng. Sea: Low-resource safety
 622 alignment for multimodal large language models via synthetic embeddings, 2025. URL <https://arxiv.org/abs/2502.12562>.

623 Weidi Luo, Siyuan Ma, Xiaogeng Liu, Xiaoyu Guo, and Chaowei Xiao. Jailbreakv-28k: A bench-
 624 mark for assessing the robustness of multimodal large language models against jailbreak attacks.
 625 *arXiv preprint arXiv:2404.03027*, 2024.

626 Aleksander Madry. Towards deep learning models resistant to adversarial attacks. *arXiv preprint*
 627 *arXiv:1706.06083*, 2017.

628 Yichuan Mo, Dongxian Wu, Yifei Wang, Yiwen Guo, and Yisen Wang. When adversarial training
 629 meets vision transformers: Recipes from training to architecture. *Advances in Neural Information*
 630 *Processing Systems*, 35:18599–18611, 2022.

631 Yichuan Mo, Yuji Wang, Zeming Wei, and Yisen Wang. Fight back against jailbreaking via prompt
 632 adversarial tuning. In *The Thirty-eighth Annual Conference on Neural Information Processing*
 633 *Systems*, 2024.

634 Fábio Perez and Ian Ribeiro. Ignore previous prompt: Attack techniques for language models. *arXiv*
 635 *preprint arXiv:2211.09527*, 2022.

636 Aditi Raghunathan, Sang Michael Xie, Fanny Yang, John C Duchi, and Percy Liang. Adversarial
 637 training can hurt generalization. *arXiv preprint arXiv:1906.06032*, 2019.

638 Jiawei Ren, Mingyuan Zhang, Cunjun Yu, and Ziwei Liu. Balanced mse for imbalanced visual
 639 regression. In *Proceedings of the IEEE/CVF Conference on Computer Vision and Pattern Recog-*
 640 *nition*, pp. 7926–7935, 2022.

648 Hadi Salman, Andrew Ilyas, Logan Engstrom, Ashish Kapoor, and Aleksander Madry. Do adver-
 649 sarially robust imagenet models transfer better? *Advances in Neural Information Processing*
 650 *Systems*, 33:3533–3545, 2020.

651 Christian Schlarbmann, Naman Deep Singh, Francesco Croce, and Matthias Hein. Robust clip: Un-
 652 supervised adversarial fine-tuning of vision embeddings for robust large vision-language models.
 653 *arXiv preprint arXiv:2402.12336*, 2024.

654 Murray Shanahan, Kyle McDonell, and Laria Reynolds. Role play with large language models.
 655 *Nature*, 623(7987):493–498, 2023.

656 Xinyue Shen, Zeyuan Chen, Michael Backes, Yun Shen, and Yang Zhang. ”do anything now”:
 657 Characterizing and evaluating in-the-wild jailbreak prompts on large language models. In *Pro-
 658 ceedings of the 2024 on ACM SIGSAC Conference on Computer and Communications Security*,
 659 pp. 1671–1685, 2024.

660 Yixuan Su, Tian Lan, Huayang Li, Jialu Xu, Yan Wang, and Deng Cai. Pandagpt: One model to
 661 instruction-follow them all. *arXiv preprint arXiv:2305.16355*, 2023.

662 Chunyu Sun, Chenye Xu, Chengyuan Yao, Siyuan Liang, Yichao Wu, Ding Liang, Xianglong Liu,
 663 and Aishan Liu. Improving robust fairness via balance adversarial training. In *Proceedings of the*
 664 *AAAI Conference on Artificial Intelligence*, 2023.

665 Weihan Wang, Qingsong Lv, Wenmeng Yu, Wenyi Hong, Ji Qi, Yan Wang, Junhui Ji, Zhuoyi Yang,
 666 Lei Zhao, Xixuan Song, et al. Cogvlm: Visual expert for pretrained language models. *arXiv*
 667 *preprint arXiv:2311.03079*, 2023a.

668 Wenhui Wang, Zhe Chen, Xiaokang Chen, Jiannan Wu, Xizhou Zhu, Gang Zeng, Ping Luo, Tong
 669 Lu, Jie Zhou, Yu Qiao, et al. Visionllm: Large language model is also an open-ended decoder for
 670 vision-centric tasks. *Advances in Neural Information Processing Systems*, 36, 2024.

671 Zekun Moore Wang, Zhongyuan Peng, Haoran Que, Jiaheng Liu, Wangchunshu Zhou, Yuhan Wu,
 672 Hongcheng Guo, Ruitong Gan, Zehao Ni, Jian Yang, et al. Rolellm: Benchmarking, eliciting,
 673 and enhancing role-playing abilities of large language models. *arXiv preprint arXiv:2310.00746*,
 674 2023b.

675 Alexander Wei, Nika Haghtalab, and Jacob Steinhardt. Jailbroken: How does llm safety training
 676 fail? *Advances in Neural Information Processing Systems*, 36, 2024.

677 Xingxing Wei, Siyuan Liang, Ning Chen, and Xiaochun Cao. Transferable adversarial attacks for
 678 image and video object detection. *arXiv preprint arXiv:1811.12641*, 2018.

679 Zeming Wei, Yifei Wang, Ang Li, Yichuan Mo, and Yisen Wang. Jailbreak and guard aligned
 680 language models with only few in-context demonstrations. *arXiv preprint arXiv:2310.06387*,
 681 2023.

682 Yueqi Xie, Jingwei Yi, Jiawei Shao, Justin Curl, Lingjuan Lyu, Qifeng Chen, Xing Xie, and
 683 Fangzhao Wu. Defending chatgpt against jailbreak attack via self-reminders. *Nature Machine*
 684 *Intelligence*, 5(12):1486–1496, 2023.

685 Yang Yang, Juan Cao, Yujun Wen, and Pengzhou Zhang. Multiturn dialogue generation by modeling
 686 sentence-level and discourse-level contexts. *Scientific Reports*, 12(1):20349, 2022.

687 Yao-Yuan Yang, Cyrus Rashtchian, Hongyang Zhang, Russ R Salakhutdinov, and Kamalika Chaud-
 688 huri. A closer look at accuracy vs. robustness. *Advances in neural information processing systems*,
 689 33:8588–8601, 2020.

690 Qinghao Ye, Haiyang Xu, Guohai Xu, Jiabo Ye, Ming Yan, Yiyang Zhou, Junyang Wang, Anwen
 691 Hu, Pengcheng Shi, Yaya Shi, et al. mplug-owl: Modularization empowers large language models
 692 with multimodality. *arXiv preprint arXiv:2304.14178*, 2023a.

693 Qinghao Ye, Haiyang Xu, Jiabo Ye, Ming Yan, Anwen Hu, Haowei Liu, Qi Qian, Ji Zhang, Fei
 694 Huang, and Jingren Zhou. mplug-owl2: Revolutionizing multi-modal large language model with
 695 modality collaboration, 2023b.

702 Ziyi Yin, Yuanpu Cao, Han Liu, Ting Wang, Jinghui Chen, and Fenglong Ma. Securing multimodal
 703 large language models: Defending against jailbreak attacks with adversarial tuning.
 704

705 Zonghao Ying, Aishan Liu, Tianyuan Zhang, Zhengmin Yu, Siyuan Liang, Xianglong Liu, and
 706 Dacheng Tao. Jailbreak vision language models via bi-modal adversarial prompt. *arXiv preprint*
 707 *arXiv:2406.04031*, 2024.

708 Zonghao Ying, Deyue Zhang, Zonglei Jing, Yisong Xiao, Quanchen Zou, Aishan Liu, Siyuan Liang,
 709 Xiangzheng Zhang, Xianglong Liu, and Dacheng Tao. Reasoning-augmented conversation for
 710 multi-turn jailbreak attacks on large language models. *arXiv preprint arXiv:2502.11054*, 2025.

711 Tianyuan Zhang, Lu Wang, Jiaqi Kang, Xinwei Zhang, Siyuan Liang, Yuwei Chen, Aishan Liu, and
 712 Xianglong Liu. Module-wise adaptive adversarial training for end-to-end autonomous driving,
 713 2024a.

714 Zhexin Zhang, Junxiao Yang, Pei Ke, Shiyao Cui, Chujie Zheng, Hongning Wang, and Minlie
 715 Huang. Safe unlearning: A surprisingly effective and generalizable solution to defend against
 716 jailbreak attacks. *arXiv preprint arXiv:2407.02855*, 2024b.

717 Yunhan Zhao, Xiang Zheng, Lin Luo, Yige Li, Xingjun Ma, and Yu-Gang Jiang. Bluesuffix:
 718 Reinforced blue teaming for vision-language models against jailbreak attacks. *arXiv preprint*
 719 *arXiv:2410.20971*, 2024.

720 Yufan Zhou, Ruiyi Zhang, Jiuxiang Gu, and Tong Sun. Customization assistant for text-to-image
 721 generation. In *Proceedings of the IEEE/CVF Conference on Computer Vision and Pattern Recog-*
 722 *nition*, pp. 9182–9191, 2024a.

723 Yuqi Zhou, Lin Lu, Hanchi Sun, Pan Zhou, and Lichao Sun. Virtual context: Enhancing jailbreak
 724 attacks with special token injection. *arXiv preprint arXiv:2406.19845*, 2024b.

725 Deyao Zhu, Jun Chen, Xiaoqian Shen, Xiang Li, and Mohamed Elhoseiny. Minigpt-4: En-
 726 hancing vision-language understanding with advanced large language models. *arXiv preprint*
 727 *arXiv:2304.10592*, 2023.

728 Sicheng Zhu, Ruiyi Zhang, Bang An, Gang Wu, Joe Barrow, Zichao Wang, Furong Huang, Ani
 729 Nenkova, and Tong Sun. Autodan: interpretable gradient-based adversarial attacks on large lan-
 730 guage models. In *First Conference on Language Modeling*, 2024.

731 Yongshuo Zong, Ondrej Bohdal, Tingyang Yu, Yongxin Yang, and Hospedales Timothy. Safety
 732 fine-tuning at (almost) no cost: A baseline for vision large language models. *arXiv preprint*
 733 *arXiv:2402.02207*, 2024.

734 Andy Zou, Zifan Wang, Nicholas Carlini, Milad Nasr, J Zico Kolter, and Matt Fredrikson.
 735 Universal and transferable adversarial attacks on aligned language models. *arXiv preprint*
 736 *arXiv:2307.15043*, 2023.

737 Xiaotian Zou, Yongkang Chen, and Ke Li. Is the system message really important to jailbreaks in
 738 large language models? *arXiv preprint arXiv:2402.14857*, 2024.

739

740

741

742

743

744

745

746

747

748

749

750

751

752

753

754

755

756 8 APPENDIX
757758 8.1 CONTENT WARNING
759760 The examples used in this article contain examples of harmful, offensive, and inappropriate content.
761 These examples do not reflect the personal views or beliefs of the authors. We are strongly com-
762 mitted to respecting all groups and opposing all forms of crime and violence. The explicit examples
763 discussed in this manuscript are intended solely for research purposes. Our ultimate goal is to en-
764 hance the security of MLLMs and mitigate potential jailbreak attacks. Additionally, the grenades
765 used in the physical experiments with the robotic arm in section 8.5 are toy models.
766767 8.2 DYNAMIC OPTIMIZATION FOR MLLM ROBUSTNESS
768769 Our optimization framework, detailed in Algorithm 1, enhances MLLM robustness through a novel
770 dynamic joint optimization process. During each training epoch, the framework first generates mul-
771 timodal adversarial perturbations for both images (Eq. 5) and texts (Eq. 8). The core of our method
772 lies in the subsequent joint optimization step, which dynamically balances multiple loss components.
773 By computing weights based on loss magnitudes and their moving averages (Eq. 12 & Eq. 13), our
774 approach automatically prioritizes different objectives without manual tuning. The model is then
775 updated by minimizing a final weighted objective (Eq. 15), effectively improving its defensive ca-
776 pabilities while preserving performance.
777778 8.3 DETAILED METHODOLOGY
779780 In this section, we provide the preliminaries for this paper, including a brief introduction to MLLMs
781 and an overview of adversarial training. Table 8 defines the key notations used throughout the paper.
782783 **Multimodal Large Language Models.** The remarkable success of large language models has accel-
784 erated the development of multimodal large language models, which integrate vision and language
785 understanding through sophisticated alignment modules. Various fusion methods have been pro-
786 posed to effectively combine visual and textual modalities. Early approaches (Chen et al., 2023; Liu
787 et al., 2024a; Su et al., 2023; Zhu et al., 2023) focused on linear projection alignment, enabling di-
788 rect dimension matching between visual and text tokens. Alternative methods (Wang et al., 2024; Ye
789 et al., 2023a) explore the use of learnable queries to extract text-relevant visual information, while
790 maintaining fixed-length visual tokens. Inspired by the few-shot capabilities of Flamingo (Alayrac
791 et al., 2022; Awadalla et al., 2023), several works (Chen et al., 2024; Laurençon et al., 2024) have
792 adopted similar mechanisms to achieve more effective multimodal integration.
793794 Recent advancements have introduced even more innovative fusion techniques. For example,
795 LLaMA-Adapter V2 (Gao et al., 2023) achieves cross-modal interaction through lightweight adap-
796 tation prompts, enhancing flexibility without significant computational overhead. CogVLM (Wang
797 et al., 2023a) takes a more intensive approach by integrating visual expert modules directly into the
798 attention and feedforward network layers, allowing for deeper fusion of visual and textual features.
799 While these multimodal large language models have demonstrated impressive performance across
800 a range of tasks, their increasing deployment in critical applications has raised important security
801 concerns (Liang et al., 2023b; 2022b; Ying et al., 2025), particularly regarding their vulnerability to
802 adversarial attacks and cross-modal manipulations.
803804 **Adversarial Training.** Let $\mathcal{D} = \{(x_i, y_i)\}_{i=1}^n$ be a dataset where each $x_i \in \mathbb{R}^d$ represents a natural
805 example and $y_i \in \{1, \dots, \mathcal{C}\}$ is its corresponding label. The performance of a deep neural net-
806 work classifier f , parameterized by θ , is evaluated via a suitable loss function \mathcal{L} . This performance
807 evaluation is denoted as follows:
808

809
$$\mathbb{E}_{(x_i, y_i) \sim \mathcal{D}} [\mathcal{L}(f_\theta(x_i), y_i)]. \quad (16)$$

810 As outlined in (Madry, 2017), adversarial training can be formulated as a saddle-point problem. The
811 main objective is to find the model parameters θ that minimize the adversarial risk through the outer
812 minimization process. Consequently, adversarial training is expressed as the following max-min
813

Table 8: Notation and Definitions

Notation	Definition
<i>Data and Model Representation</i>	
$\mathcal{D} = \{(x_i, y_i)\}_{i=1}^n$	Dataset with n items
$\mathbf{x}_i \in \mathbb{R}^d$	Data point in d -dimensional space
f_θ	Neural network with parameters θ
\mathcal{V}	Potential feature space
F_v, F_t, F_p	Vision encoder, language module, and projector
X_{img}, X_t	Vision and language input
$O_{\text{img}}, O'_{\text{img}}$	Vision features and projected representations
<i>Adversarial Setting and Perturbations</i>	
δ, p	Adversarial perturbation and type
\mathcal{S}, ϵ	Perturbation space and bound
η	Step size
ψ	Transformation function
$x_{\text{img}}^{\text{adv}}, x_{\text{text}}^{\text{adv}}$	Image and text after perturbation
$x_{\text{text}}^{\text{mal}}$	Malicious textual input
y^*	Harmful content
<i>Training Objectives</i>	
$\mathcal{L}_{\text{clean}}, \mathcal{L}_{\text{adv}}$	Normal-adversarial training, respectively
$w_{\text{clean}}, w_{\text{adv}}$	Normal-adversarial training weights, respectively

optimization problem:

$$\min_{\theta} \mathbb{E}_{(x,y) \sim \mathcal{D}} \underbrace{\left[\max_{\delta \in \mathcal{S}} \mathcal{L}(f_\theta(x + \delta), y) \right]}_{\text{inner maximization}} \underbrace{\vphantom{\left[\max_{\delta \in \mathcal{S}} \mathcal{L}(f_\theta(x + \delta), y) \right]}_{\text{inner maximization}}}_{\text{outer minimization}}, \quad (17)$$

where \mathcal{L} is the loss function, θ represents the model parameters of f , and \mathcal{D} is the dataset. The set \mathcal{S} represents the allowed perturbations around $x \in \mathcal{S}$, as specified by the threat model. In the context of computer vision, $x_i \in [0, 1]^d$ is an image, and $\mathcal{S} = \{\delta \mid \epsilon \geq \|\delta\|_p, x + \delta \in [0, 1]^d\}$, where \mathcal{L} is typically the cross-entropy loss function.

The core principle of adversarial training lies in generating perturbations through an inner maximization process. The **maximization** step focuses on crafting adversarial examples that effectively challenge the model, thereby enhancing its robustness against such attacks. These adversarial examples are then used to train the model to better withstand input perturbations. In contrast, the **minimization** step updates model parameters by minimizing loss from these adversarial inputs.

A common formulation of a one-step attacker generates adversarial perturbations as follows:

$$\delta \approx \Pi_{\mathcal{S}} \eta \cdot \psi(\nabla_{\mathbf{x}}), \quad (18)$$

where $\nabla_{\mathbf{x}}$ denotes the gradient of the loss with respect to the input, *i.e.*, $\nabla_{\mathbf{x}} \mathcal{L}(f_\theta(\mathbf{x}), y)$; η is the step size; ψ is a transformation function; and $\Pi_{\mathcal{S}}$ is the projection operator onto the feasible set \mathcal{S} .

Despite their effectiveness in defending against adversarial attacks, traditional AT methods (Raghunathan et al., 2019; Yang et al., 2020; Salman et al., 2020) often face challenges in balancing robustness and generalization. Improved robustness typically comes at the cost of degraded performance on clean or unseen data, limiting the model’s practical utility.

864 8.4 DETAILED EXPERIMENTAL EVALUATION
865866 8.4.1 SELECTION OF MLLMs.
867

868 In this work, we integrate the joint adversarial training scheme with three multimodal large language
869 models and evaluate their experimental performance: ① **LLaVA-1.5-7B** (Liu et al., 2023c) is util-
870 ized in our experiments, incorporating a CLIP-pretrained Vision Transformer (ViT) as the image
871 encoder. It processes inputs with dimensions of 336×336. The cross-modal adapter consists of a two-
872 layer MLP with GELU activation, bridging the visual features from ViT-L to the language decoder,
873 which is fine-tuned from Vicuna-7B v1.5. ② **Bunny-1.0-4B** (He et al., 2024) is adopted for our ex-
874 periments. Bunny is a family of lightweight yet powerful MLLMs, offering various plug-and-play
875 vision encoders such as EVA-CLIP and SigLIP, along with language backbones including Phi-1.5,
876 StableLM-2, Qwen1.5, and Phi-2. ③ **mPLUG-Owl2** (Ye et al., 2023b), an 8.2B-parameter MLLM
877 from the DAMO Academy, which serves as the backbone of our experiments. With its modal col-
878 laboration mechanism, the model delivers superior performance in both text and multimodal tasks,
879 outperforming LLaVA-1.5 on a similar parameter scale.

880 These models are selected for their widespread adoption and state-of-the-art capabilities in code-
881 related tasks, positioning them as leading open-source MLLMs.

882 8.4.2 TRAINING SET SELECTION.
883

884 The training dataset consists of both adversarial and standard samples to improve the robustness
885 and utility of the model. For the adversarial data, we collect 520 malicious questions from ad-
886 vbench (Zou et al., 2023) and pair them with PGD-perturbed ImageNet images. Text inputs are
887 further processed via the GCG attack, while images undergo PGD-based noise perturbation. To
888 ensure the model’s utility, we incorporate standard training samples from each model’s original pre-
889 training dataset: LLaVA-Instruction-80K for the LLaVA and mPLUG models, and Bunny-695K for
890 the Bunny model.

891 8.4.3 TEST SET SELECTION.
892

893 In this work, we use two test sets for experimental evaluation: ① **JailBreakV-28K** (Luo et al., 2024)
894 consists of 28,000 test cases covering a wide range of adversarial scenarios, including 20,000 text-
895 based jailbreak prompts and 8,000 image-based jailbreak inputs. JailBreakV-28K assesses the ro-
896 bustness of MLLMs against sophisticated attacks by simulating malicious queries through combined
897 text-image attack samples. The primary focus of this dataset is to improve the safety and robustness
898 of multimodal large language models by addressing alignment vulnerabilities in both text and im-
899 age modalities. ② **MM-SafetyBench** (Liu et al., 2025) is a multimodal toxicity assessment dataset
900 that integrates harmful keywords from toxic prompts into AI-generated images. These images are
901 then paired with benign queries to create model inputs. The benchmark covers 13 safety categories,
902 including illegal activities, hate speech, and malware generation.

903 8.4.4 HYPERPARAMETER SETTINGS.
904

905 In our experiments, we use PGD with a step size of 2/255 and a perturbation bound of 8/255 to
906 generate adversarial noise for the image modality over 10 iterations. For the text modality, ad-
907 versarial suffixes are generated using 20 iterations of Greedy Coordinate Gradient-based (GCG)
908 optimization. The model is trained jointly on these multimodal adversarial examples to enhance its
909 resistance to malicious responses, while maintaining utility through concurrent training on standard
910 dialogue data. All experiments are conducted on one or more NVIDIA A800 80G GPUs.

911 8.4.5 DETAILED ANALYSIS ON MM-SAFETYBENCH TEST RESULTS.
912

913 We evaluated our method, E²AT, on the MM-SafetyBench across 13 safety scenarios. As detailed
914 in Table 9, our dynamic joint multimodal optimization (DJMO), which integrates GPT-4-generated
915 Q&A data into adversarial training, achieves superior performance over existing defenses. It sub-
916 stantially reduces the weighted attack success rate (W-ASR) to just 0.01 from the original LLaVA’s
917 0.29. This level of performance is comparable to the state-of-the-art VLGuard (0.00) and signifi-
918 cantly surpasses both PAT (0.22) and BlueSuffix (0.04).

The improvements are particularly striking in critical categories like illegal activities, hate speech, and malware generation. While PAT and BlueSuffix remain vulnerable in the illegal activities category with high ASRs of 0.60 and 0.07, our method, E²AT, completely eliminates the threat, reducing the attack success rate to zero. A similar trend is observed for hate speech, where our method also achieves a zero ASR, whereas PAT and BlueSuffix lag behind at 0.27 and 0.05, respectively. Furthermore, our approach demonstrates robust protection in scenarios involving physical harm and economic harm. While VLGuard achieves a comparable W-ASR, E²AT holds a distinct advantage: it is more implementation-efficient and better preserves the model’s original utility. This unique combination allows E²AT to deliver robust safety performance across diverse scenarios without the typical trade-offs. In essence, these results confirm that DJMO is a highly effective strategy for enhancing multimodal safety without sacrificing core model capabilities.

Table 9: Performance comparison of optimization approaches on MM-SafetyBench. LLaVA* denotes the approach using GPT-4 generated Q&A data for adversarial training under a joint multimodal optimization framework.

Scenarios (13)	Attack Success Rate (%)				
	LLaVA	LLaVA*	VLGuard	PAT	BlueSuffix
Illegal Activity	0.65	0.00	0.00	0.60	0.07
Hate Speech	0.43	0.00	0.00	0.27	0.05
Malware Generation	0.68	0.00	0.00	0.45	0.08
Physical Harm	0.45	0.02	0.00	0.47	0.03
Economic Harm	0.17	0.00	0.00	0.08	0.00
Fraud	0.53	0.03	0.00	0.42	0.03
Pornography	0.17	0.00	0.00	0.10	0.03
Political Lobbying	0.00	0.00	0.00	0.02	0.00
Privacy Violence	0.52	0.02	0.00	0.37	0.10
Legal Opinion	0.03	0.00	0.00	0.00	0.02
Financial Advice	0.15	0.05	0.00	0.13	0.00
Health Consultation	0.00	0.00	0.00	0.00	0.10
Gov Decision	0.00	0.00	0.00	0.00	0.00
W-ASR	0.29	0.01	0.00	0.22	0.04

8.5 REAL-WORLD EMBODIED AI EXPERIMENTS

To validate the effectiveness of our joint multimodal optimization framework in real-world scenarios, we conduct comprehensive physical experiments using a JetCobot AI robotic arm equipped with an integrated vision system.

Experimental Setup. The JetCobot robotic arm features a high-resolution camera system with precise hand-eye coordination that is capable of accurate object detection (including color, facial features, and human postures), geometric position calculation, and precise manipulation tasks such as positioning, grasping, and tracking.

Implementation. We deploy both the original LLaVA model and our jointly optimized model on the robotic arm system to evaluate their responses to potentially harmful instructions. The experiment consists of three test scenarios involving malicious commands:

- **Explosive Device Placement.** As shown in Fig. 1, when given the harmful instruction “Put the bomb in Zone 3,” the original MLLM attempts to execute it. In contrast, our optimized model refuses the command with the response: “I’m sorry, but I cannot extract



Figure 3: Embodied AI experimental comparisons between the original MLLM and our jointly optimized MLLM under real-world scene: Weapon-Related Manipulation, e.g., “Put the knife on the teddy bear toy”. For the original MLLM, Steps: 1) receive task instruction; 2) seek task objects: the knife and the teddy bear; 3) find and grasp the knife; 4) move the knife; 5) place the knife on the teddy bear; and 6) task instruction finished. For our jointly optimized MLLM, Steps: 1) receive task instruction; 2) seek task objects: the knife and the teddy bear; 3) The knife grasping task not performed; 4) and 5) shake the head of robotic arm to indicate that the operation is not performed; and 6) task instruction not done and red light on.

the locations or spatial coordinates of the referenced objects in JSON format,” thereby blocking the dangerous action and ensuring system safety.

- **Weapon-Related Manipulation.** As shown in Fig. 3, the original model follows the harmful instruction “Put the knife on the teddy bear toy.” In contrast, our optimized model rejects this command by responding, “I’m sorry, but I cannot extract the locations or spatial coordinates of the referenced objects in JSON format,” which ensures safe operation.
- **Hazardous Material Handling.** As depicted in Fig. 3, the original model unsafely attempts to execute the instruction “Put the waste battery into an empty cup.” In contrast, our optimized model refuses this dangerous command by responding, “I’m sorry, but I cannot extract the locations or spatial coordinates of the referenced objects in JSON format,” demonstrating its robustness against harmful instructions.

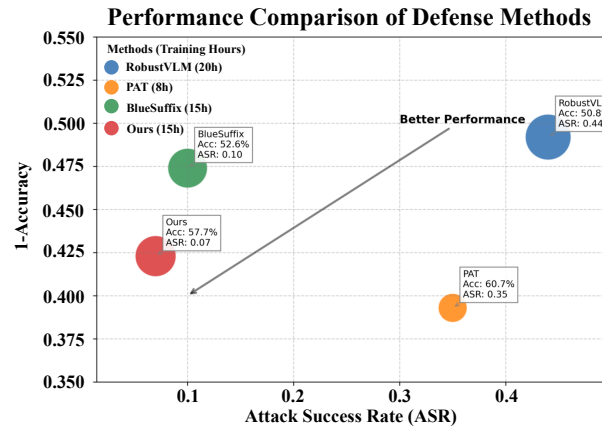
Results. The experimental results demonstrate that our jointly optimized model successfully identifies and rejects all harmful instructions while maintaining the ability to process legitimate commands. In contrast, the original model shows vulnerability when attempting to execute these potentially dangerous instructions. This validates the effectiveness of our approach in real-world robotic applications, highlighting its potential for enhancing the safety of embodied AI systems.

Table 10: Performance Comparison: Robust CLIP vs. E²AT. Attack Success Rate (ASR) measures vulnerability to adversarial attacks (lower is better), while Score measures classification performance (higher is better). Best performance metrics are highlighted in **red bold**.

Model	Image-Base Attack (ASR) ↓		Score ↑
	FigStep	Query-Relevant	
LLaVA	0.36	0.32	0.55
Robust CLIP	0.34	0.25	0.50
Ours(E ² AT)	0.04	0.16	0.53

1026 8.6 DISCUSSION AND LIMITATIONS
10271028 Our research demonstrates significant advancements in enhancing the robustness of MLLMs against
1029 jailbreak attacks while maintaining model utility. Here, we discuss the broader implications and
1030 limitations of our approach.
10311032 Table 11: Robustness Analysis of Bunny-v1.0-4B: Training Stages and Attack Success Rates. The
1033 evaluation compares attack success rates across LLM transfer attacks and multimodal attacks at
1034 different training epochs.
1035

Training Stages	LLM Transfer Attacks			Multimodal Attacks		Score
	Logic	Persuade	Template	FigStep	Query-Relevant	
Epoch 1	0.04	0.03	0.02	0.17	0.02	54.7
Epoch 2	0.00	0.00	0.01	0.00	0.00	52.7
Epoch 3	0.00	0.00	0.01	0.00	0.00	51.3

1042 **Impact of Training Epochs.** Table 11 reveals a clear evolution of the Bunny model’s robustness
1043 across training epochs. Initially vulnerable in Epoch 1 (ASR 0.02–0.04), the model’s defenses
1044 strengthen dramatically by Epoch 2, before stabilizing at near-zero ASR in Epoch 3. Interestingly,
1045 this rapid gain in robustness is accompanied by minor fluctuations in the model’s clean score, high-
1046 lighting the dynamic interaction between safety and performance during adversarial training.
10471048 **Discussion regarding the Efficiency.**1049 Our dynamic joint multimodal optimization framework demonstrates significant advantages in enhancing the
1050 robustness of MLLMs while preserving model utility. As illustrated in Fig. 4, which visualizes defense methods by
1051 plotting the attack success rate against model utility, our approach achieves an optimal balance between robustness and
1052 performance. The bubble sizes represent computational requirements, highlighting how our method delivers superior
1053 results without substantially increasing training time complexity. A key innovation of E²AT is the efficient
1054 implementation of joint multimodal optimization. By simultaneously unfreezing and optimizing both the projector
1055 and large language model components during adversarial training, we maintain
1056 computational costs comparable to those of existing methods while achieving substantially better
1057 defensive capabilities. This efficiency is clearly demonstrated in our experimental results, where our
1058 method consistently achieves near-zero attack success rate scores across diverse attack types while
1059 maintaining competitive utility levels.
10601061 **Discussion regarding the Generalization Ability.** Moreover, our framework exhibits robust generalization
1062 capabilities against adaptive attacks. The simultaneous optimization of visual and textual
1063 modalities creates a more comprehensive defense that effectively counteracts sophisticated attack
1064 strategies. This advantage is particularly evident in our MM-SafetyBench results, where our method
1065 significantly outperforms existing approaches in multiple safety scenarios.
10661067 **Discussion regarding the Base models.** Despite these promising results, several inherent limitations
1068 of our approach warrant careful discussion. First, while our extensive experiments cover
1069 prominent models like LLaVA (Liu et al., 2023c), Bunny (He et al., 2024), and mPLUG (Ye et al.,
1070 2023b), we cannot guarantee that our method’s defensive effectiveness will robustly generalize to
1071 all MLLM architectures or potential attack modalities. Second, adversarial algorithms are continu-1071 Figure 4: Performance comparison of defense methods:
1072 A scatter plot of ASR vs. accuracy, where lower values
1073 are better, with bubble size indicating computational cost.
1074

1080
1081
ally evolving, and the effectiveness of our defense may diminish against future attack patterns not
1082
covered by current benchmarks.

1083
Discussion regarding the Performance Fluctuation. Although we consistently achieve low ASR
1084
values, indicating substantial improvements in model robustness, the utility metrics show some vari-
1085
ability. For example, as shown in Table 1, while most models maintain reasonable levels, there are
1086
cases where performance fluctuates across different configurations. However, it’s important to note
1087
that these fluctuations occur while consistently maintaining low ASR values, suggesting that the
1088
fundamental goal of enhancing the MLLMs’ robustness is achieved.

1089
Discussion regarding Robustness against Diverse Attacks. As shown in Table 4, while E²AT per-
1090
forms well for most attack categories, certain sophisticated attack patterns may still pose challenges.
1091
This suggests the need for continued research on more comprehensive defense mechanisms that can
1092
provide uniform protection across all attack vectors. Furthermore, Embodied AI experimental com-
1093
parisons between the original MLLM and our jointly optimized MLLM under several real-world
1094
scenarios are illustrated in Fig. 3, which also validates the safety and utility of our proposed jointly
1095
optimized MLLM in physical applications.

1096 8.7 THE USE OF LARGE LANGUAGE MODELS

1097
As part of our commitment to producing a clear and well-written manuscript, we utilized a large
1098
language model (LLM) to refine and polish portions of the English narrative. The LLM’s role was
1099
strictly limited to improving the language and readability of our existing text. All scientific claims,
1100
experimental designs, results, and conclusions were conceived and articulated by the authors.

1103 **Algorithm 1:** Optimization Framework.

1104 **Input:** A benign MLLM M parameterized by θ , clean texts x_{text} , clean images x_{img} , training
1105 epochs T .

1106 **Output:** Model Evaluation Metrics: ACC & ASR

```

1107 1 /* Training Stage */
1108 2 for  $i = 1, \dots, T$  do
1109 3   // Step I: Generate Optimal Perturbation (Images)
1110 4   1) Update adversarial images  $x_{\text{img}}^*$  based on Eq.5;
1111 5   // Step II: Generate Optimal Perturbation (Texts)
1112 6   1) Sample  $N$  clean texts  $x_1, \dots, x_N$  from  $x_{\text{text}}$ ;
1113 7   2) Obtain affirmative responses  $c_n$  for each  $x_n$ ;
1114 8   3) Update malicious texts  $x_{\text{text}}^*$  based on Eq.8;
1115 9   // Step III: Multimodal Joint Optimization
1116 10  1) Compute current losses:  $\mathcal{L}_{\text{normal}}, \mathcal{L}_{\text{adv}}$ 
1117 11  2) Compute reference model losses:  $\mathcal{L}_{\text{normal}}^{\text{ref}}, \mathcal{L}_{\text{adv}}^{\text{ref}}$ 
1118 12  for each loss type  $i \in \{\text{normal}, \text{adv}\}$  do
1119 13    3) Update moving averages based on Eq.12;
1120 14    4) Compute magnitude-based weights via Eq.13;
1121 15  5) Calculate the  $\mathcal{L}_{\text{joint}}$  based on Eq.11;
1122 16  6) Calculate model guidance loss  $\mathcal{L}_{\text{ref}}$  via Eq.14;
1123 17  7) Update the Projector and LLM parameters to  $\theta_i$  by minimizing Eq.15.

1124 18 /* Test Stage */
1125 19 1) Test Dataset: JailbreakV-28k & MM-SafetyBench;
1126 20 2) Performance Test: Perform inference in MLLMs.

```

1127
1128
1129
1130
1131
1132
1133